High resolution synchrotron FTIR spectroscopy of the ν_{11} bending vibrational fundamental transition of dimethylsulfoxyde (DMSO) in the far IR frequency range at 380 cm^{-1}

Arnaud Cuisset[a,*], Lia Nanobashvili (ლია ნანობაშვილი)[a,b], Irina Smirnova[a,c], Robin Bocquet[a], Francis Hindle[a], Gaël Mouret[a], Olivier Pirali[d,e], Pascale Roy[d], Dmitriĭ A. Sadovskiĭ[a]

[a] *Laboratoire de Physico-Chimie de l'Atmosphère, UMR CNRS 8101, Université du Littoral – Côte d'Opale, 59140 Dunkerque, France*
[b] *Department of Exact and Natural Sciences, Graduate Program in Electrical and Electronic Engineering, Ivane Javakhishvili Tbilisi State University, Tbilisi, Georgia*
[c] *Physical Faculty of the M. V. Lomonosov Moscow State University, Moscow, Russia*
[d] *Synchrotron* SOLEIL, *L'orme des Merisiers, Saint-Aubin - BP48, 91192 Gif-sur-Yvette, France*
[e] *Laboratoire de Photophysique Moléculaire, CNRS, Bât. 210, Universit Paris–Sud, 91405 Orsay Cedex, France*

Abstract

We report on the first successful high-resolution gas phase study of the "parallel" band of DMSO at 380 cm^{-1} associated with the ν_{11} bending vibrational mode. The spectrum was recorded at 0.0015 cm^{-1} resolution using the AILES beamline of the SOLEIL synchrotron source, the IFS 125 FTIR spectrometer and a multipass cell allowing an optical path of 150 m. The rotational constants and centrifugal corrections obtained from the analysis of the resolved rotational transitions reproduce the spectrum to the experimental accuracy.
`DMSOnu11` 2010-03-05 12:33 © 2010 Arnaud Cuisset

Keywords: synchrotron FTIR spectroscopy, THz radiation, vibration-rotation spectrum, bending mode, accidental symmetric top, effective rotational Hamiltonian
PACS: 33.20.Ea, 33.20.Vq, 33.15.Mt

1. Introduction

Dimethylsulfoxyde (DMSO) is an excellent solvating agent which has many important applications in chemistry, biochemistry and industry. In the ocean atmosphere, DMSO is naturally emitted from the oxidation of dimethylsulfide (DMS) produced by the marine phytoplankton and plays a significant role in the atmospheric sulfur chemistry [2]. Furthermore, DMSO is considered to be an organosulfide simulant of toxic agents such as the mustard gas. So in addition to its importance for industrial and environmental studies, monitoring DMSO concentrations is of considerable interest to civil protection.

First spectroscopic analysis of the microwave (mw) transitions in the ground state of DMSO which allowed

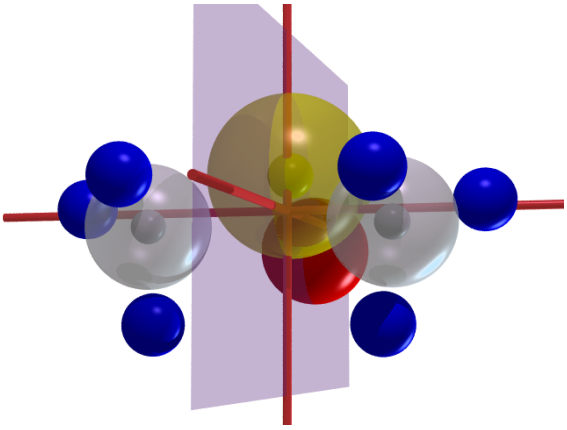

Figure 1: Schematic representation of the equilibrium configuration of DMSO according to the *ab initio* computation using [1]; axes correspond to the three principal axes of inertia crossing at the center of mass, axes *B* and *C* (vertical) lie in the the symmetry plane.

*Corresponding author
Email addresses: `Arnaud.Cuisset@univ-littoral.fr` (Arnaud Cuisset), `sadovski@univ-littoral.fr` (Dmitriĭ A. Sadovskiĭ)

to determine quartic centrifugal distortion constants was reported in [3, 4] and later again in [5]. Most comprehensively, up to $J = 50$, the ground state has been recently re-analyzed in [6]. The last reported experiments on gas phase rovibrational spectra of DMSO go back more thirty years [7] and were limited to low resolution and wavenumbers above 600 cm^{-1}. The harmonic force field of DMSO was determined by Typke and Dakkouri in 2000 [8] using liquid phase data for the low frequency bending modes, and using vibrational satellite bands in the mw region for the torsional modes with predicted frequencies below 300 cm^{-1}.

It is in this context that the first gas phase high resolution Far-InfraRed (FIR) spectroscopic analysis of DMSO was undertaken recently in [9]. This work made full use of the exceptional properties of the AILES beamline of the SOLEIL synchrotron in the THz/FIR domain [10, 11]. In the present paper, we report on the first successful analysis of the gas phase rovibrational transition involving one of the lowest frequency vibrational modes of DMSO.

DMSO is a 10-atomic C_s symmetric molecule, whose equilibrium configuration is shown in fig. 1. This average structure was derived by Typke and Dakkouri [8] after combining available data from IR, Raman and mw spectroscopy, and gas electron diffraction with *ab initio* predictions and reevaluating the harmonic force field of the molecule. Our preliminary experiments performed with the internal sources of the IFS125 Bruker FTIR spectrometer [12] allowed to update the experimental vibrational frequencies of all the IR active modes of DMSO (cf fig. 2) and to obtain a better agreement with the force field developed in [8].

At low vibrational excitations, the two methyl groups of DMSO cannot rotate internally and the vibrations of the molecule can be analyzed in terms of 24 normal modes [8]. A number of these modes, notably the symmetric (A'-type) ν_{11} and the asymmetric (A''-type) ν_{23} related to the bending vibrations of the OSC_2 frame, have frequencies in the THz domain and are strongly dipole active. However, up until now, the rotational structure of these states could not be studied due to the very low vapor pressure of DMSO and low intensity of the conventional radiation sources in this frequency domain.

2. Experimental details

Taking advantage of the natural high brilliance and the small divergence of the synchrotron radiation (SR) in the THz/FIR domain can reduce drastically the acquisition time of the rovibrational spectra [13]. Several synchrotron facilities, notably the Canadian Light Source, the Australian synchrotron, the SOLEIL synchrotron facility, and others have different IR beamlines that can be used for high resolution spectroscopy [14, 15]. This field is under rapid development.

The absorption spectra of DMSO have been recorded in the 20–600 cm^{-1} spectral range on the FIR beamline AILES of SOLEIL. Opened to external users at the end of 2008, AILES has already demonstrated its exceptional suitability for gas phase high resolution THz spectroscopy in a number of studies [16–18] which for the most part could not be performed with thermal sources. In our present study, the synchrotron radiation was absolutely essential in order to observe, in a limited time, the resolved rovibrational FIR spectrum of DMSO.

The AILES beamline was designed to obtain exceptional performances in terms of flux, spectral range, and stability in the entire IR domain. Roy et al. have developed a reliable high resolution spectroscopic ensemble providing high detection sensitivity in a wide frequency range [10]. Comparison with classical thermal sources showed that the main gain from the use of the SR was obtained in the THz/FIR spectral domain. According to the recent comparative measurements in the 100 cm^{-1} region [11], the delivered flux and the achieved S/N ratio for the SR are factor of 40 higher than those of a conventional thermal source, such as the mercury discharge lamp.

In our experiments, the AILES beamline was focused onto the entrance aperture of a high resolution Bruker IFS 125 Fourier transform interferometer containing a 6 μm mylar-Silicon composite beamsplitter suitable for the THz spectral range. In order to limit the absorption due to the atmospheric compounds, the interferometer was continuously evacuated to 10^{-5} Torr. The detector was a helium-cooled silicon bolometer equipped with an optical band-pass filters, with band widths of 10–600 cm^{-1}. DMSO of stated purity higher than 97% from Aldrich Chemical Co was used, without further purification, by direct injection of the saturated vapor pressures at room temperature in the cell (0.42 Torr at 293 K). Due to the low volatility of the compound, a high sensitivity was required for these experiments. Therefore, the spectrometer was connected to a multipass cell (in a White type configuration) adjusted to reach a 150 m optical path length. This cell was isolated from the interferometer by 50 μm thick polypropylene windows.

The observed spectrum associated with the ν_{11} rovibrational transition of DMSO is shown in fig. 2. The spectrum was recorded with the resolution $\Delta\nu = 0.0015$ cm^{-1} at a pressure of 0.06 Torr. To achieve a S/N ratio

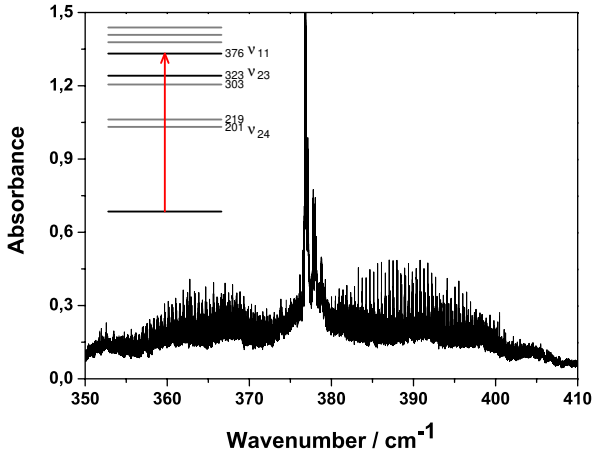

Figure 2: Spectrum of the ν_{11} fundamental band of DMSO observed using the AILES beamline of the SOLEIL synchrotron ($P = 0.06$ Torr, $L = 150$ m, $\Delta\nu = 0.00015$ cm^{-1}, 700 scans, 46 hours of acquisition). The insert (top left) shows the system of the lowest vibrational energy levels of DMSO in cm^{-1} according to our measurements and, for the two lowest modes, to [8]. Gray lines represent nearly dipole inactive states and their overtones, the arrow shows the ν_{11} transition observed in this work.

> 100 in the ν_{11} region, we had to co-add the Fourier transform of 700 interferograms. The total acquisition time amounted to 46 hours. Note that with conventional sources, several months would be necessary to obtain a similar S/N ratio! The spectrum in fig. 2 was calibrated using residual water absorption lines whose wavenumbers were taken from the HITRAN spectroscopic database [19]. The calibration accuracy was about 0.00015 cm^{-1}(RMS). For clarity, the residual water lines were subsequently removed manually from the spectrum presented in fig.2. On the other hand, the baseline was not subtracted.

3. Specifics of the rotational structure of DMSO

DMSO is a slightly asymmetric top molecule with two nearly equal rotational constants $A \gtrsim B$, and significantly smaller third constant C. Its asymmetry parameter

$$\kappa = 1 - 2\varepsilon^2 = \frac{2B - (A + C)}{A - C} \approx 0.91, \qquad (1)$$

is close to that of an *oblate* symmetric top ($\kappa = 1$). This specificity of DMSO was mentioned in [4] and the example of DMSO was used to discuss K-doubling and Watson's S-reduction [4, 20, 21].

Figure 3 illustrates the classical rotational energy of DMSO in the ground state $|0\rangle$ which is obtained after

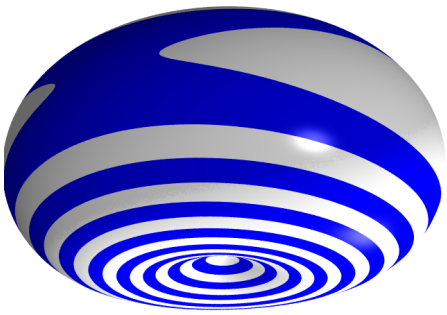

Figure 3: Classical rotational energy of DMSO in the vibrational ground state $|0\rangle$ with $J = 25$. The energy (to a fixed constant) is given by the radial distance from the origin of the plot. The surface is drawn in slightly rotated coordinates (J_a, J_b, J_c) of fig. 1. Equidistant levels of constant energy are stripe painted to display more clearly the shape of the surface. We see a deep minimum along the J_c axis (vertical) and a very shallow relief in the equatorial area with a small white maximal energy domain of stable classical rotation about axis J_a.

replacing the components (J_a, J_b, J_c) of the angular momentum operator $\mathbf{J}$ for their classical analogs

$$(J_a, J_b, J_c) = \|\mathbf{J}\|\,(\cos\theta,\ \sin\theta\,\sin\phi,\ \sin\theta\,\cos\phi).$$

Here $\|\mathbf{J}\| = \sqrt{J(J+1)}$ is given by the quantum number J, and (θ, ϕ) define coordinates on the reduced rotational phase space $\mathbb{S}^2_J$. We can see that most of $\mathbb{S}^2_J$ is taken up by stable rotations about axis C which correlate to those in the oblate symmetric top limit (concentric stripes in fig. 3). Rotations about axis A are represented by a much smaller domain of $\mathbb{S}^2_J$ (white area near axis J_a in the equatorial belt of the surface), and a similarly small domain (self-intersecting blue stripe in fig. 3) corresponds to delocalized unstable motions with energies between those of the C and A rotations. To appreciate how close the molecule is to the symmetric top limit, imagine [22] switching the ^{16}O atom for its isotope ^{17}O or ^{18}O. In the usual DMS^{16}O (fig. 1), axis A, or the stable principal axis with minimal moment of inertia, is the axis *perpendicular* to the symmetry plane. DMS^{17}O is very close to the symmetric top, and in DMS^{18}O axes A and B are interchanged, and the stable axis lies *in-plane*.

Given that (in the simplest rigid rotor approximation) the relative area of the A-domain of $\mathbb{S}^2_J$ is

$$\frac{2}{\pi}\arcsin\varepsilon = \frac{2}{\pi}\arcsin\sqrt{\frac{A-B}{A-C}} \approx 0.14,$$

the number of quantum states localized in that domain, or *A-states*, is below 10–15% of all states. Furthermore, since localized states form doublets, the number of the latter can be estimated as $\approx 0.14\,J$ and so they exist

only for $J > 8$. The rest of the states are the C-states which correlate with the oblate symmetric top states and which are classified adequately by the good quantum number $K = K_c$ of J_c. For this reason, axis C is the most natural choice of the quantization axis for the rotational basis functions $|J, K\rangle$ used to construct the matrix of the effective rotational Hamiltonian $H(\mathbf{J})$.

Recall that to minimize the number of adjustable parameters in H, the latter is reduced to a D_2-symmetric form following the procedure by Watson [23]. This form is not unique and for nearly symmetric tops, it is customary [4, 20, 21, 24] to use the s-form because it requires a smaller transformation and so is, in principle, a faster converging series. Additionally, one may also expect a lesser distortion of the original dipole moment operator. This all may be beneficial to the initial stages of the spectroscopic analysis and to higher J extrapolations.

In practice, however, the situation is less straightforward. In addition to a scalar series in J^2, the s-form Hamiltonian includes diagonal and tensorial terms. The former are various powers of K^2 (or $\cos^2\theta$) and contribute primarily to the energies of the C-states, while the latter include also powers of $(J_a \pm \mathrm{i}J_b)^2$ (or $\sin^2\theta$) that describe the A-states or the intermediate states. The number of terms of each kind is roughly equal, while the number of C states is much larger. This disproportion may result in stronger correlations between the tensorial terms, especially when the A-states are observed with lower precision or not observed at all. In such cases, the a-form may turn out more stable [6].

4. Analysis of the ν_{11} fundamental

In our present analysis, we treated the $|\nu_{11} = 1\rangle$ fundamental as an isolated vibrational state, i.e., we considered no explicit Coriolis interactions with other close lying states, notably the $|\nu_{23} = 1\rangle$ fundamental, and no vibrational resonances, such as the Fermi resonance with the $|\nu_{24} = 2\rangle$ overtone (cf fig. 2 and [8]). This turned out to be sufficient within the accuracy of our data and the range of the observed J values. In our approximation, the effective rovibrational Hamiltonian

$$H = \omega_{11}v + (A + v\delta A)J_x^2 + (B + v\delta B)J_y^2 + (C + v\delta C)J_z^2 + \ldots$$

includes purely rotational terms describing the ground state and their corrections in the upper state $|v = 1\rangle$. For the higher order terms in H, we used Watson's s-form with axis z the axis C of the oblate symmetric top limit. As discussed in sec. 3, such choice is the most physical for DMSO. Moreover, we had the advantage of observing sufficiently many transitions to the A-states in order to stabilize the s-form in the least square fit.

The initial analysis and assignments became possible after observing that the $|0\rangle \rightarrow |\nu_{11} = 1\rangle$ was quite similar to a parallel band of a symmetric top molecule: a

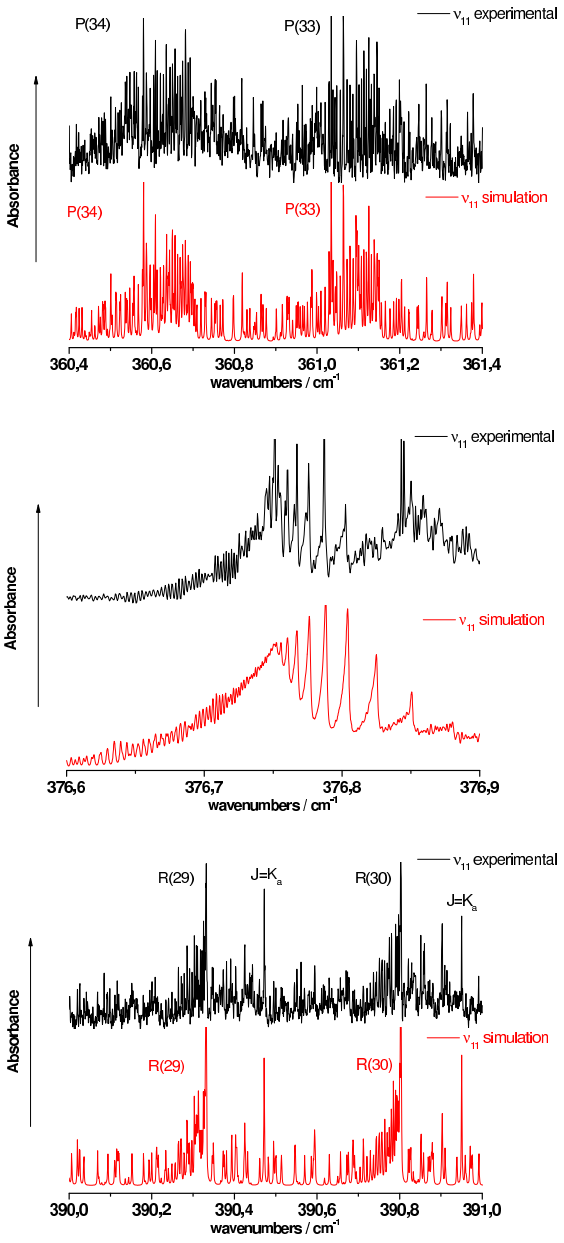

Figure 4: Fragments of the observed and calculated spectra of the ν_{11} band of DMSO; top to bottom P-branch, Q-branch, and R-branch. The predicted spectra are simulated using the Lorentzian profile with HWHM of 0.0008 cm^{-1}.

strong Q-branch shouldered by weaker and reasonably regular P- and R-branches (see fig. 2). This meant that out of the two components of the in-plane dipole moment $\mu(q) = (0, \mu_b, \mu_c)^T q$ induced by this A'-symmetric vibration, the C-component (that would be responsible for a parallel transition in the symmetric top) was stronger. At closer look (see fig. 4), the band had a complex, dense, and unresolved Q-branch, which extended far enough to obscure the low-J multiplets of the P-branch, while the beginning of the R-branch was buried under additional dense bands, possibly hot bands, off the high frequency head of the Q-branch. Nevertheless, entering basic rotational and dipole moment parameters, we managed to model several P- and R-branch $J = 12 \ldots 15$ multiplets well enough for picking combination frequencies and making unambiguous assignments. After that, fitting the spectrum became relatively straightforward. We used the programs by Pickett [25, 26] for computing and fitting the spectra and the programs by Kisiel [27, 28] to assist assignments.

Combining the mw $|0\rangle \rightarrow |0\rangle$ data from [6] and our FIR measurements on $|0\rangle \rightarrow |1\rangle$, we adjusted all parameters in H and reproduced the experimental data close to their estimated experimental accuracy, see table 1 and fig. 5. To this end it was necessary to develop H to degree 8 in (J, K). Figure 5 shows that we have been able to reach all levels within assigned J-multiplet, and in particular levels of type A at the high energy end. The latter was possible due to the strong transitions to the topmost A-state doublet with $K_a = \pm J$ which could be observed very clearly at the blue edge of R multiplets, see fig. 4.

The resulting parameter values are given in table 1 and the measured transitions in the P and R branches of the band ν_{11} are given as supplementary materials in sec. Appendix A. Because the accuracy of the mw data was 0.03 MHz while that of the FIR data was about 5 MHz, the resulting $|0\rangle$ parameters were only but slightly affected by the FIR combination frequencies, and are close to those obtained in [6] for their S-III choice.

We can see in fig. 5 that the rotational structure of $|\nu_{11} = 1\rangle$ is standard. In fact, in the scale of the figure it differs invisibly from that of $|0\rangle$. There is no qualitative complications due to the closeness of the symmetric top limit. In fact the two methyl groups are too bulky and this hinders the decrease of the CSC angle when the molecule rotates about axis A. So the angle remains far from ≈ 90 degrees and the geometry is sufficiently far from that of the accidental symmetric top. The only problem that we encountered was the persistent strong local perturbation of a single C-type $K = 15$ or 16 level in each multiplet starting with $J = 30$ (see gaps in fig. 5). Additionally, we registered a small number of relatively weak and sparse lines that did not belong to our ν_{11} band. The perturbed level sequence had to be excluded from our fit and its neighbors exhibited characteristically increasing systematic errors as they approached the perturber. These errors may have resulted in a slightly higher overall discrepancy of the fit compared to the estimated experimental uncertainty.

Table 1: Parameters of the effective rotational Hamiltonian for the ground state and the ν_{11} fundamental state of DMSO. Also provided is the summary of the experimental data used for each state, the accuracy σ_{calc} of the fit, and the number of lines reproduced with errors outside the $2\sigma_{\text{calc}}$ interval.

$\|0\rangle$		$\|\nu_{11} = 1\rangle$		
		ω_{11}	11294.71934(72)	GHz
A	7036.58255(19)	δA	5.0427(80)	MHz
B	6910.83024(19)	δB	3.6235(81)	MHz
C	4218.77665(27)	δC	−1.0061(68)	MHz
$-D_K$	−3.99040(47)	$-\delta D_K$	0.193(29)	KHz
$-D_{JK}$	8.93877(55)	$-\delta D_{JK}$	−0.451(36)	KHz
$-D_J$	−6.08972(36)	$-\delta D_J$	0.299(16)	KHz
d_1	−0.163670(63)	δd_1	0.066(11)	KHz
d_2	−0.271802(33)	δd_2	0.0443(75)	KHz
H_K	−0.02233(50)	δH_K	0.044(39)	Hz
H_{JKK}	0.05486(70)	δH_{JKK}	−0.141(74)	Hz
H_{JJK}	−0.04143(56)	δH_{JJK}	0.196(57)	Hz
H_J	0.00946(28)	δH_J	−0.089(18)	Hz
h_1	−0.002260(72)	δh_1	−0.027(14)	Hz
h_2	0.001283(70)	δh_2	−0.030(13)	Hz
h_3	−0.001384(23)	δh_3	−0.0060(39)	Hz
L_J	−0.000181(79)	δL_J	0.0293(67)	mHz
L_{JJK}	0.00089(21)	δL_{JJK}	−0.122(26)	mHz
L_{JK}	−0.00123(43)	δL_{JK}	0.244(48)	mHz
L_{KKJ}	0.00032(50)	δL_{KKJ}	−0.263(43)	mHz
L_K	0.00007(25)	δL_K	0.108(18)	mHz
l_1	0.000243(32)	δl_1	0.0123(58)	mHz
l_2	−0.000139(36)	δl_2	0.0161(59)	mHz
l_3	0.000034(17)	δl_3	0.0048(30)	mHz
l_4	−0.0000059(35)	δl_4	−0.00060(49)	mHz
lines	1717 mw		1581 FIR	
	807 FIR freq. diff.			
J	1 . . . 39		5 . . . 40	
σ_{exp}	0.03 MHz		0.00015 cm^{-1}	
σ_{calc}	0.03 MHz		0.00022 cm^{-1}	
$\mathcal{N}_{>2\sigma}$	101 mw		36 FIR	

5. Conclusion

It is always a matter of considerable satisfaction to participate in a fresh important development in a field where such advancement seemed unlikely just a few years ago. Together with several other recent studies [13–16], our successful measurement and analysis of

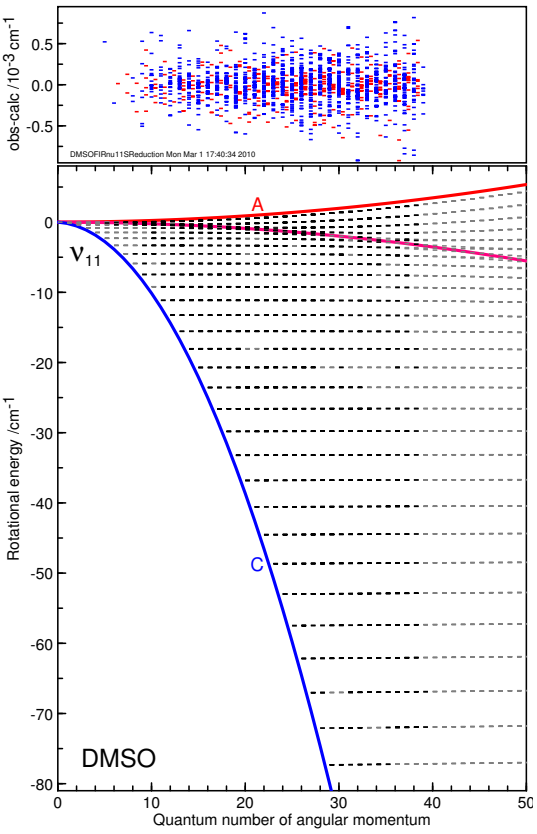

Figure 5: Rotational energy levels (main panel) of DMSO in the vibrational state ν_{11} according to parameters in table 1. Energies are shown minus the scalar energy $H_s(J)$; bold solid lines represent energies of classical stationary axes of rotation (relative equilibria), observed levels are marked red. Small upper panel shows respective errors in reproducing rotational transitions in the ν_{11} FIR band. Color version: red and blue represent *A*- and *C*-type levels respectively.

the ν_{11} band of DMSO demonstrates most convincingly the potential of the synchrotron spectroscopy in the far IR. The use of the synchrotron radiation made suddenly available for spectroscopic studies a great number of new subjects.

Thus our present work is just at the beginning of unraveling the rovibrational structure of low frequency bending and torsional vibrational states of DMSO and yielding important comprehensive structural and spectroscopic information on this molecule. The next natural step in this study will be the analysis of the "perpendicular" ν_{23} band which was observed in the same experiment [9]. This analysis may be complicated by a possibly strong Coriolis interaction with another close vibrational state (see the scheme in fig. 2).

It is also tempting to investigate further the nature of the perturbing state mentioned in sec. 4. The little available information may suggest a "dark" state situated within 15 cm^{-1} below $|\nu_{11} = 1\rangle$. From fig. 2 and taking into account that harmonic frequencies [8] used to draw fig. 2 are uncertain and anharmonic corrections may ran as high as 10–15 cm^{-1}, we may deduce that such a state may well be an $|\nu_{24} = 2\rangle$ overtone coupled to $|\nu_{11} = 1\rangle$ via a cubic Fermi term or q^3J Coriolis terms. Finally, in the same context, it is interesting to understand fully the origin of the other band(s) whose weaker *Q*-branch(es) is(are) observed in our experiment (see fig. 4). These may be related to hot bands, to perturbing states, or even to aggregates of DMSO with itself or with water and other impurities. We anticipate substantial progress in answering these questions in the near future.

Acknowledgments

We thank B. I. Zhilinskiĭ for discussions and encouragement and D. Balcon, J. B. Brubach and M. Rouzières of the AILES group at SOLEIL for their help during experiments; Lia Nanobashvili is grateful to LPCA and ULCO for financial support and assistance during her stay in France. We thank Margulès et al. for providing their mw data prior to the final publication of [6]. This work was partially funded by the Délégation Générale pour l'Armement (projet de Recherche Exploratoire et Innovation n^o 06.34.037).

Appendix A. Supplementary data

Supplementary data associated with this letter can be found in the online version, at ...

References

[1] M. J. Frisch, et al., Computer program Gaussian 03, Rev. D.01, Gaussian, Inc., Wallingford, CT, 2004.
[2] O. Boucher, C. Moulin, S. Belviso, O. Aumont, L. Bopp, E. Cosme, R. von Kuhlmann, M. G. Lawrence, M. Pham, M. S. Reddy, J. Sciare, C. Venkataraman, Atmos. Chem. Phys. 3 (2003) 49–65.
[3] W. Feder, H. Dreizler, H. D. Rudolph, V. Typke, Z. Naturforsch. A 24 (1969) 266–??
[4] V. Typke, J. Molec. Spectrosc. 63 (1976) 170–9. See Table II on p. 174 for mw data on DMSO.
[5] E. Fliege, H. Dreizler, V. Typke, Z. Naturforsch. A 38 (1983) 668–75.
[6] L. Margulès, R. A. Motiyenko, E. A. Alekseev, J. Demaison, J. Molec. Spectrosc. 260 (2010) 23–9.
[7] G. Geiseler, G. Hanschmann, J. Molec. Struct. 11 (1972) 283–96.
[8] V. Typke, M. Dakkouri, J. Molec. Struct. 599 (2001) 177–93.
[9] A. Cuisset, I. Smirnova, R. Bocquet, F. Hindle, G. Mouret, C. Yang, O. Pirali, P. Roy, A.I.P Conf. Proc. 1214 (2010) 85–7. To appear in Infr. Phys & Techn.

[10] P. Roy, M. Rouzieres, Z. Qi, O. Chubar, Infr. Phys. and Techn. 49 (2006) 139–46.

[11] J. B. Brubach, L. Manceron, M. Rouziéres, O. Pirali, D. Balcon, F. K. Tchana, V. Boudon, M. Tudorie, T. Huet, A. Cuisset, P. Roy, A.I.P Conf. Proc. 1214 (2010) 81–4. To appear in Infr. Phys & Techn.

[12] A. Cuisset, G. Mouret, O. Pirali, P. Roy, C. F., N. H., J. Demaison, J. Phys. Chem. B 112 (2008) 12516–25.

[13] A. R. W. McKellar, J. Molec. Spectrosc. (2010). Accepted manuscript.

[14] A. McKellar, B. Billinghurst, J. Molec. Spectrosc. 260 (2010) 66–71.

[15] T. Chimdi, E. G. Robertson, L. Puskar, C. D. Thompson, M. J. Tobin, D. McNaughton, Chem. Phys. Lett. 465 (2008) 203–6.

[16] V. Boudon, O. Pirali, P. Roy, J.-B. Brubach, L. Manceron, J. Vander Auwera, J. Quant. Spectrosc. Rad. Transf. (2010).

[17] D. Jacquemart, L. Gomez, N. Lacome, J. Y. Mandin, O. Pirali, P. Roy, J. Quant. Spectrosc. Rad. Transf. (2010).

[18] F. Kwabia Tchana, J. M. Flaud, W. J. Lafferty, L. Manceron, P. Roy, J. Quant. Spectrosc. Rad. Transf. (2010).

[19] L. S. Rothman, et al., J. Quant. Spectrosc. Rad. Transf. 110 (2009) 533–72.

[20] D. Papousek, M. R. Aliev, Molecular vibrational-rotational spectra, volume 17 of *Studies in Phys. and Theor. Chem.*, Elsevier, Amsterdam, 1982. For asymmetric top molecules see Chap. III.17 on p. 160.

[21] V. Typke, J. Molec. Struct. 384 (1996) 35–40.

[22] B. Zhilinskií, 2010. Private communication.

[23] J. K. G. Watson, in: J. R. Durig (Ed.), Vibrational Spectra and Structure, volume 6, Elsevier, 1977, pp. 1–89.

[24] M. R. Aliev, J. K. G. Watson, in: K. N. Rao (Ed.), Molecular Spectroscopy - Modern Research, volume III, Academic Press, 1985, pp. 1–67.

[25] H. M. Pickett, J. Molec. Spectrosc. 148 (1991) 371–7.

[26] H. M. Pickett, SPFIT/SPCAT programs for vibration-rotation spectra, 2007. For more information and examples see also `http://www.ph1.uni-koeln.de/cdms/pickett` and `http://info.ifpan.edu.pl/~kisiel/asym/pickett/crib.htm`.

[27] Z. Kisiel, ASCP/SVIEW programs for graphical assignments of vibration-rotation spectra, 2009. For applications see [28].

[28] Z. Kisiel, L. Pszczólkowski, I. R. Medvedev, M. Winnewisser, F. C. D. Lucia, E. Herbst, J. Molec. Spectrosc. 233 (2005) 231–43.